Strong localization of light and photonic atoms

S.C. Rand

Abstract: In the strong localization regime, light confined to a well-defined volume of space by the mutual interference of its countless constituent scattered waves can be expected to acquire unusual characteristics. These include a vanishing momentum, an effective tensorial rest mass, and "photonic atom recoil." Impurity atoms that emit light under these conditions should consist of coupled atom–cavity systems with energy densities extending over regions larger than the atoms, but smaller than a cubic wavelength, in which radiant transport is suppressed by near-field correlated scattering. This unusual regime is now accessible over broad wavelength ranges in random nanoparticle media, opening the way to studies of novel phenomena such as strong localization phase transitions, lasers without cavities, and optical energy storage.

PACS Nos.: 78.45+h, 78.60Hk, 42.55Rz, 42.25Fx, 78.35+c, 78.20Dj, 42.50Gy

Résumé: En régime de forte localisation nous attendons que la lumière qui est confinée à un volume bien défini de l'espace par l'interférence du très grand nombre de ses ondes constituantes diffusées acquiert des caractéristiques inhabituelles. Ceux-ci peuvent inclure une vitesse de groupe nulle, un tenseur de masse au repos efficace et un « recul atomique photonique ». Les atomes d'impureté qui émettent de la lumière sous ces conditions, devraient se comporter comme des systèmes couplés atome–cavité, avec des densités d'énergie s'étendant sur des régions plus grandes que les atomes, mais plus petites que le cube d'arête égale à la longueur d'onde et dans lequel le transport radiatif est supprimé par la diffusion en champ proche. Ce mécanisme inhabituel est maintenant accessible sur un grand domaine de longueurs d'onde dans des média à très faible densité aléatoire d'impuretés, ce qui ouvre la voie à l'étude de nouveaux phénomènes, comme les transitions de phase fortement localisées, les lasers sans cavité et le stockage d'énergie optique.

[Traduit par la rédaction]

1. Introduction

We describe some interesting implications and prospects related to recent experiments on continuous-wave powder lasers in highly scattering rare-earth media.[1] It seems altogether fitting some twenty-two years after being involved with Brillouin scattering experiments under the guidance of Professor Stoicheff, that this contribution to a special issue celebrating his remarkable leadership and achievements in teaching and research should touch on new aspects of light scattering in random media that have

[1] G. Williams, S.C. Rand, T. Hinklin, and R.M. Laine. Laser action in strongly scattering rare-earth-doped dielectric nanophosphors. Manuscript in preparation.

Received January 15, 2000. Accepted April 19, 2000. Published on the NRC Research Press Web site on August 30, 2000.

S.C. Rand. Division of Applied Physics, Randall Laboratory, University of Michigan, Ann Arbor, MI 48109-1120, U.S.A. Telephone: (734) 763-6810; FAX: (734) 647-2718; e-mail: scr@eecs.umich.edu

recently become the focus of research by our group at the University of Michigan in Ann Arbor. Scattering was a key topic in the exciting mix of spectroscopy and nonlinear optics projects that took place in the Stoicheff laboratory at the University of Toronto over many decades. At that time the interest was mostly in using light as a precise tool to probe highly ordered materials. In this paper, we explore very much the opposite theme, by considering how the structure and composition of highly scattering, random media can influence the nature of light itself, and provide new evanescent light sources and energy storage possibilities.

It is well known that light is both wavelike and particlelike. However, we do not ordinarily associate with photons such properties as a quasi-particle "size" with subwavelength dimensions, an effective rest mass, or a vanishing propagation velocity in all three dimensions. Nor do we typically encounter situations in which a stationary electromagnetic field may itself be a source of propagating photons. These and other novel aspects of light–matter interactions can nevertheless be expected as consequences of strong, multiple scattering in lossless media when the mean free transport distance l^* is considerably less than a wavelength. When $l^* \ll \lambda$, for example, in an ultrafine powder far from absorptive resonances, the coherence length is also subwavelength and light becomes evanescent or nonpropagating.[1] This is a consequence of the wave equation itself, which in this limit does not support propagating wave solutions. In this regime, new coherence and scattering phenomena are expected to arise that can be probed and controlled electrically or optically — including omnidirectional laser emission and dynamic energy storage in the coupled states of randomly scattered light localized around impurity atoms, which we refer to here as "photonic atoms." Consequently, the interaction of light with random nanoparticle media offers exciting new horizons in optical science.

2. Theory

We first examine some consequences of multiple scattering and derive a criterion for strong localization. Consider a lossless random medium in which electromagnetic radiation is found to scatter so strongly in a random fashion that it propagates less than a wavelength on average before becoming directionally randomized. Subwavelength localization requires a subwavelength coherence length, since destructive interference must be effective on the scale of the wavelength ($l^* < \lambda$). Elastic scattering in this limit therefore produces a *nonpropagating* wave that is evanescent [1] as the result of total internal reflection (provided absorption is negligible). Reflected, evanescent waves are the consequence of a negative dielectric constant, and appear, for example, at the boundary of dense and light media and in plasmas at frequencies below the plasma frequency ω_p. Their characteristic, exponential decay is induced by boundary scattering. This situation is quite distinct from the exponential decay associated with internal degrees of freedom (damping/absorption) within the medium, and it is helpful to review the mechanisms whereby a field decays, within the unified context of a simple damped-harmonic-oscillator model.

The relative permittivity $\varepsilon_r(\omega)$ can readily be calculated from the equation of motion of an electron oscillator damped at a rate γ and driven by a field $E(r, t) = E_0 \exp[i(Kr - \omega t)]$. The standard result is

$$\varepsilon_r(\omega) = (n + i\kappa)^2 = 1 + \frac{\omega_p^2(\omega_0^2 - \omega^2)}{(\omega_0^2 - \omega^2)^2 + \gamma^2\omega^2} + \frac{2i\gamma\omega\omega_p^2}{(\omega_0^2 - \omega^2)^2 + \gamma^2\omega^2} \tag{1}$$

Here n and κ are the real and imaginary parts of the complex refractive index that determine wave vector $k = \sqrt{\varepsilon_r(\omega)}k_0$, and the plasma frequency is defined as usual by $\omega_p^2 = Ne^2/\varepsilon_0 m_e$ where e and m_e are the charge and rest mass of the electron, respectively. In an absorptive medium, the damping of the oscillator yields a nonzero imaginary component κ of k in (1) that results in exponential decay of the wave according to $E(r, t) = E_0 \exp[i(nk_0 r - \omega t)] \exp[-\kappa k_0 r]$. In a lossless medium both γ and κ are zero, but exponential decay of the wave can still occur whenever the (real) dielectric constant is negative. This can be illustrated by setting $\gamma = 0$ in (1), and taking the system resonant frequency to

be low ($\omega_0 \to 0$). This yields the plasma dispersion relation

$$\varepsilon_r(\omega) = 1 - \frac{\omega_p^2}{\omega^2} \tag{2}$$

Notice that ε_r is negative when $\omega_p/\omega > 1$, yielding a field of the form

$$E(r, t) = E_0 \exp(-i\omega t) \exp(-k_0 r \sqrt{(\omega_p^2/\omega)^2 - 1})$$

for which we ordinarily define an attenuation length or range r^* according to $k_0 r^* \sqrt{(\omega_p^2/\omega)^2 - 1} = 1$. Using the latter expression (valid only for $\omega_p/\omega > 1$) we can relate the permittivity to r^*.

$$\left(\frac{\omega_p}{\omega}\right)^2 = 1 + \left(\frac{1}{k_0 r^*}\right)^2 \tag{3}$$

It is well known that radiation of frequency $\omega < \omega_p$ reflects *externally* from plasmas [2]. However, total reflection also occurs for radiation generated in the *interior* of a lossless medium with a negative effective dielectric constant, provided the extent of the medium exceeds the range parameter r^*. Radiation emerging from a point source then continuously reflects back to the origin, usually on the distance scale of a few wavelengths or so, as determined by $k_0\sqrt{\varepsilon_r}$. Conversely, when the attenuation length is less than a wavelength in a lossless medium, whether this is due to total internal reflection at a boundary between two dielectrics, or to a wave impinging on a plasma below the plasma frequency, or to strong scattering in a random medium, we may infer the presence of evanescent waves and a negative dielectric constant. As we now show, the occurrence of a subwavelength range ($r^* < \lambda$) has another interesting consequence, namely, the appearance of an effective rest mass for photons in the medium.

The dispersion relation is $k^2 = \omega^2 \epsilon_r / c^2$, with ε_r given by (2) when the medium is lossless. For, light, this can be written

$$\hbar^2\omega^2 = c^2\hbar^2k^2 + \hbar^2\omega_p^2 \tag{4}$$

For comparison, the relativistic expression for the energy W of massive particles [2] is

$$W^2 = c^2p^2 + m^2c^4 \tag{5}$$

Taking into account the linear momentum of photons $p = \hbar k$, and substituting (3) in (4), we identify an effective mass for the photon from (5) equal to

$$m_{\text{eff}} = \frac{\hbar\omega}{c^2}\left[1 + \left(\frac{\omega_p^2}{\omega^2} - 1\right)\right]^{1/2} \tag{6a}$$

or, when expressed in terms of the range parameter,

$$m_{\text{eff}} = \frac{\hbar\omega}{c^2}\left[1 + \left(\frac{1}{k_0 r^*}\right)^2\right]^{1/2} \tag{6b}$$

To this point our model has not explicitly included scattering. As shown next though, these results do carry over to multiple scattering systems in which the frequency-dependent permittivity is similar to that of the simple oscillator. Notice that in the absence of reflective attenuation $r^* = \infty$, and (6b) reduces to the usual mass–energy relation $\hbar\omega = mc^2$. However, in the presence of strong reflection $r^* \to 0$, we find an effective mass contribution that is inversely proportional to r^* and exceeds the free

propagation value. This second term in (6a) and (6b) is purely a consequence of distributed (lossless) attenuation within the medium.

With no approximation as to the smallness of $|\varepsilon_r - 1|$, the relative permittivity in multiple-scattering systems can exhibit the same form as in (2). In terms of $\bar{f}(k, 0)$, the normalized (vectorial) forward scattering wave amplitude at wave vector k evaluated in the medium, $\epsilon_r(\omega)$ can be written as [3]

$$\varepsilon_r(\omega) = 1 + \left(\frac{c^2 NL}{\varepsilon_0 \omega^2}\right) \hat{e}^* \cdot \bar{f}(k, 0) \tag{7}$$

if we neglect correlated scattering. Here L is a local field factor (assumed to be a real constant of order unity), $\hat{e}$ is the incident polarization, and N is the density of scatterers. In light of prior numerical proof that the propagation constant of scalar waves can abruptly become imaginary in disordered lossless elastic scattering systems [4], the range of permissible scattering amplitudes in (7) must include $\mathrm{Re}\left\{\hat{e}^* \cdot \bar{f}(k, 0)\right\} < 0$. In this range, (2) and (6) still hold, but for scattering systems we make the replacements $\omega_p \leftrightarrow \omega_s$ and $r^* \leftrightarrow \xi l^*$, where ξ is a dimensionless range-correlation ratio on the order of two, and

$$\omega_s^2 = c^2 \left(\frac{NL|\,\mathrm{Re}[\hat{e}^* \cdot \bar{f}(k, 0)]|}{\varepsilon_0}\right) \tag{8}$$

This yields a transport mean free path of

$$l^* = \frac{1}{\xi}\left(\frac{NL\,|\mathrm{Re}[\hat{e}^* \cdot \bar{f}(k, 0)]|}{\varepsilon_0 k_0^2} - 1\right)^{-1/2} \tag{9}$$

With these substitutions, the effective mass expressions given by (6a) and (6b) apply to multiple scattering systems with negative ϵ_r. The value of $m_{\mathrm{eff}} \propto (l^*)^{-1}$ depends, however, on the polarization of the light field, or its vector character in the following way. Even in a random medium consisting of dipole scatterers, the average sum of n scattered wave vectors is shorter along the polarization axis (for example, for a linear input polarization perpendicular to the scanning plane) than perpendicular to it [5]. In the diffusive regime l^* is, therefore, substantially different for different polarizations. While near-field scattering should diminish these differences, the scattering contribution to effective mass will, in general, yield a tensorial "rest" mass.

An immediate consequence of (2), (8), and the dispersion relation $k^2 = \omega^2 \varepsilon_r / c^2$ is that the group velocity vanishes whenever the permittivity becomes negative. Throughout the range $0 < \varepsilon_r < 1$, the group velocity v_g of normally dispersed light is less than c and the phase velocity v_p exceeds c. But when ε_r actually reaches zero or turns negative, the phase velocity is undefined and $\partial\omega/\partial k$ becomes imaginary. Irrespective of the detailed dependence of $\bar{f}$ on frequency, for $\varepsilon_r \leq 0$, we expect a group velocity of

$$v_g^{-1} \equiv \mathrm{Re}\left\{\frac{\partial k}{\partial \omega}\right\} \Rightarrow v_g = \mathrm{Re}\left\{c\sqrt{\varepsilon_r}\left(1 - \frac{c^2 NL}{2\omega}\left|\,\mathrm{Re}\left(\hat{e}^* \cdot \frac{\partial \bar{f}}{\partial \omega}\right)\right|\right)^{-1}\right\} = 0 \tag{10}$$

This result signals the onset of weak localization, or confinement with respect to only one dimension, since the velocity is defined relative to the direction of propagation of the incident coherent wave. Forward propagation along a one-dimensional string of scatterers in an otherwise lossless three-dimensional medium is evanescent on a distance scale determined by the density of scatterers, but in the other two dimensions scattered wave fronts are not confined at all. For "strong" localization to occur, we argue that it is critical for inertial restraint from scattering to counterbalance forward momentum of the otherwise freely propagating light wave, in all possible directions. In other words, the effective inertial mass given

by the second term in either (6a) or (6b) must equal or exceed the free photon mass given by the first term. This condition is met in (6a) when

$$\left(\frac{\omega_s}{\omega}\right)^2 \geqslant 2 \tag{11a}$$

or equivalently, in (6b), when

$$k_0 r^* \leqslant 1 \tag{11b}$$

or

$$k_0 l^* \leqslant \frac{1}{\xi} \tag{11c}$$

Equation (11a) specifies a critical value of the scattering amplitude needed to halt energy transport in all directions at a particular density N and vacuum wavelength $\lambda_0 = 2\pi/k_0$. Equation (11b) specifies this condition in terms of the effective range and (11c) converts this to a condition for l^*, that presumes ξ is known. Unlike the heuristic criterion of Ioffe and Regel [6] for strong localization of electron transport in semiconductors ($kl^* \sim 1$), this condition derives from a kinematic principle applicable to three-dimensional field distributions. Local field effects are incorporated through (8) and (9). Its implication is that when strong localization takes place, the light field oscillates in time but not in space, confined to a volume $\sim(r^*)^3$, which shrinks as the scattering rate increases.

3. Experiments

We now turn to experimental evidence that strong localization can occur in ultrafine dielectric powders, primarily as indicated by the observation of continuous laser action in nanopowders. Earlier efforts to demonstrate "random" lasers [7] in suspensions [8] and powders [9] resulted in pulsed emission in the diffusive regime. For example, a recent paper reported a pulsed semiconductor powder laser [10] that operated with relatively efficient distributed feedback from scattering. However, it exhibited directionally and spectrally nonrandom properties. By extending this type of observation to the continuous-wave domain, and achieving spatial and spectral randomization of laser output, we furnish strong evidence of enhanced internal reflectivity in ultrafine powders associated with evanescent waves in the strong scattering regime for the first time.

At long wavelengths, Rayleigh scattering is weak, so that $l^* \gg \lambda$. For shorter wavelengths, the scattering length diminishes smoothly, as λ^{-4} in the Mie limit, until the scattering cross section α reaches the "geometric" limit ($\sigma = 2\pi a^2$) at wavelengths much smaller than particle radius a. John [11] was the first to point out that, over a limited range of intermediate wavelengths, a region in which $l^* < \lambda$ might appear where strong localization could take place. John and Pang predicted that the threshold for laser action should decrease near the mobility edge [12]. Because Mie scattering becomes ineffective for particles smaller than the wavelength, most experiments to date have concentrated on high-index powders with particle sizes near a wavelength to maximize the cross section while maintaining the validity of Mie theory. However, this overlooks the potential importance of correlated scattering [13] among smaller particles at densities exceeding $1/\lambda^3$. Interparticle interference effects can enhance distributed reflectivity and high densities of scatterers ($> \lambda^{-3}$) can even relax the mobility edge condition [4]. We show below that the spectral region over which continuous laser action can be achieved seems to be surprisingly broad in ultrafine rare-earth nanopowders synthesized by Laine and co-workers [14].

Doped, rare-earth powders can be produced by low-cost pyrolysis that yields unaggregated single crystals (Fig. 1). Average particle diameters in the 10–40 nm range are readily obtained this way. This yields powder densities well in excess of $1000/\lambda^3$ and exceptionally wide coherent back-scattering

Fig. 1. Transmission electron micrograph of δ-Al_2O_3 nanoparticles synthesized by the flame spray pyrolysis method described in the text. Note the single crystal facets and separated grains.

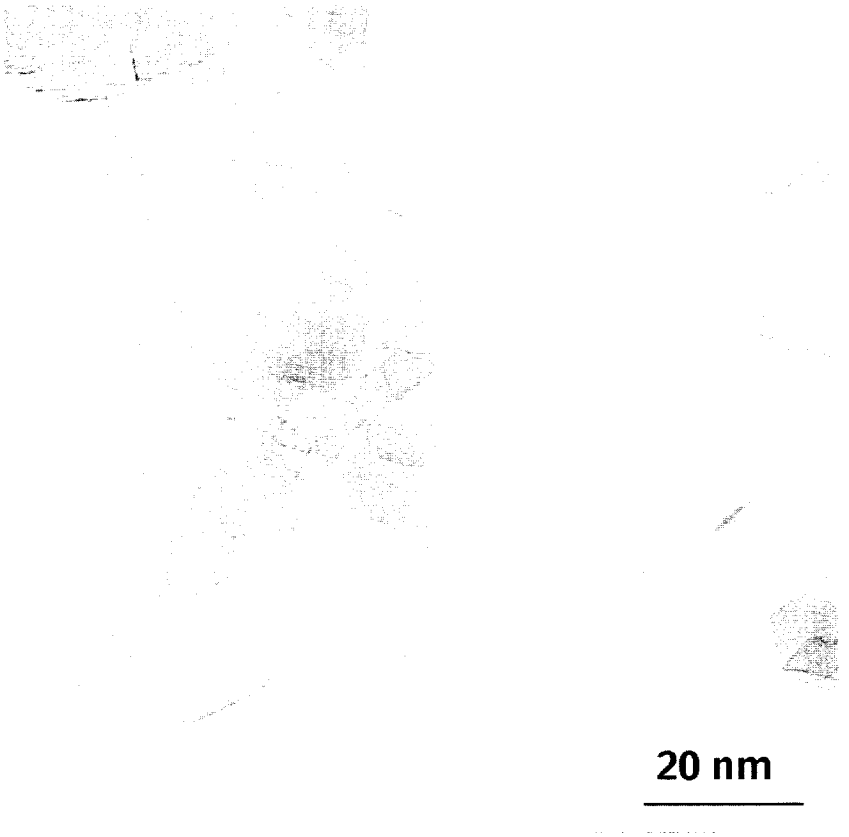

cones with comparable widths in parallel and perpendicular polarizations (Figs. 2*a* and 2*b*). In Fig. 3, cathodoluminescence data of dry Pr^{3+}:β''-Al_2O_3 powders in ultrahigh vacuum show how the intensity and spectra of the rare-earth impurity emission evolve as the electron beam current is changed. Constant accelerating voltage maintains constant electron penetration depth. In Fig. 4, output curves at different voltages are shown, indicating how output depends on the depth at which light is generated. Spectra were acquired at several angles with respect to the sample normal through chamber viewports, but were invariably the same as shown in Fig. 3. Spectral features showed no mode structure, only modest line-narrowing above the transition points,[1] and no indication of speckle in photographs covering solid angles as large as 0.038 sr.

4. Results and discussion

A key observation in this work is that abrupt changes in the output slopes – thresholds – are observed as excitation current is varied. At low voltages particularly, in the range 1–4 keV, one finds emission curves that are linear above and below a sharp transition point. This is most unexpected, but several aspects of the data presented in Fig. 4 can be understood semiquantitatively within the context of stimulated emission with distributed feedback. For example, the variation of "threshold" with voltage

Fig. 2. (*a*) Experimental back-scattered intensity versus angle at $\lambda_{ex} = 632.8$ nm (upper trace) and at $\lambda_{ex} = 362$ nm (lower trace), from Ce:δ-Al_2O_3 and Pr:β''-Al_2O_3 nanopowders, respectively (input and output polarizations perpendicular to scan plane). Contiuous curves are theoretical fits that take internal reflectivity into account [16]. (*b*) Experimental back-scattered intensity versus angle $\lambda_{ex} = 632.8$ nm from Pr:β''-Al_2O_3 nanopowders (input and output polarizations parallel to scan plane).

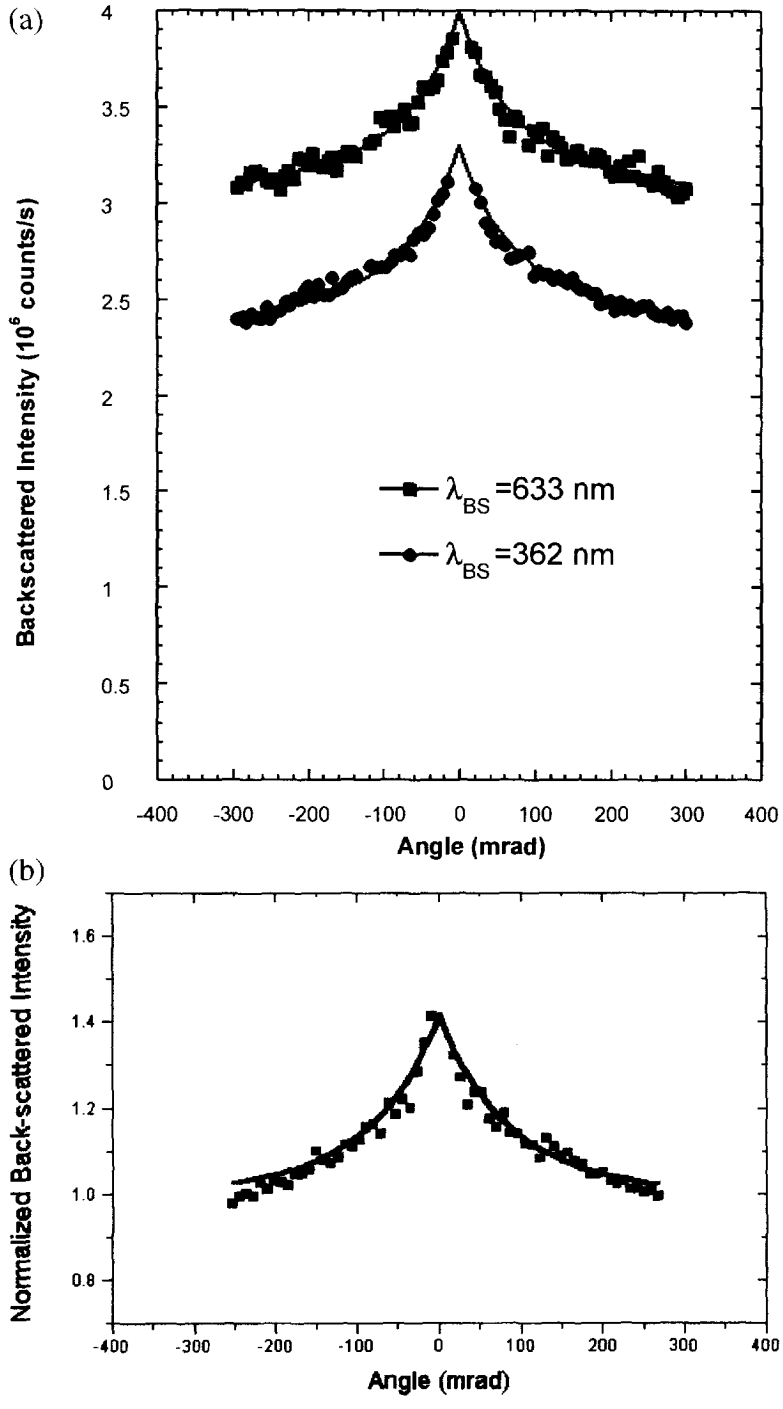

Fig. 3. Cathodoluminescence spectra of Pr^{3+}:β''-Al_2O_3 nanoparticles (ϕ = 27 nm) excited by various electron beam currents at 5 keV in a 7 mm spot-size (T = 293 K).

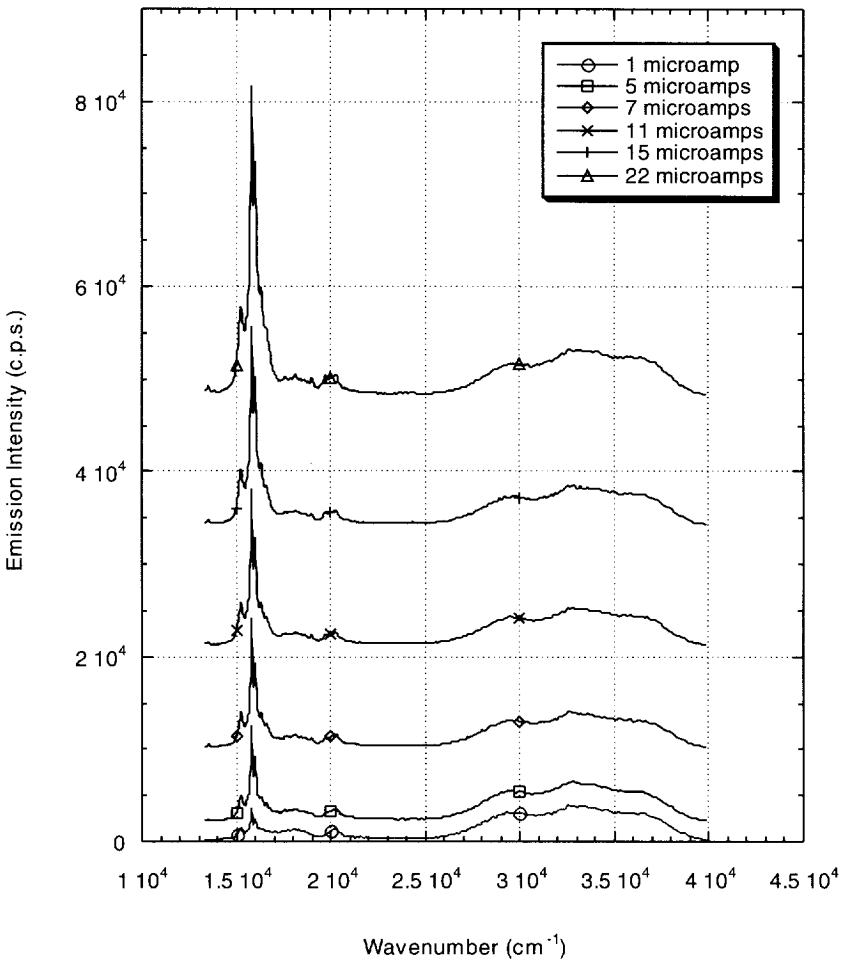

is consistent with electron penetration into the sample, since proximity of the emission source to the surface strongly affects its output coupling. A direct comparison of calculated penetration depths (Fig. 4) with the sharpest, lowest threshold curve in Fig. 4 suggests that deposition of energy at 4 keV is highly effective. The electron beam then terminates at a depth close to l^*. The generation of inverted atoms and stimulated emission at this depth can be expected to optimize excitation and output coupling simultaneously, because this produces the largest volume of excited atoms close enough to the surface for light to experience frustrated reflection.

When more energy per incident particle is available, and penetration is deeper, the output curves develop more curvature, thresholds become less well-defined, and amplification, which does not rely on feedback, appears to set in. This is consistent with the mechanism of photon escape from deep within the medium being single-pass amplification at higher voltages. Together with observations of line-narrowing, quenching of competitive transitions, and linearity of the output curves above threshold reported elsewhere,[1] our findings at voltages in the range 1–4 keV constitute strong evidence of

Fig. 4. Plots of cathodoluminescence intensity versus current in Pr^{3-}:β''-Al_2O_3 nanoparticles ($\phi = 27$ nm), at various electron beam voltages in the range 1–10 keV.

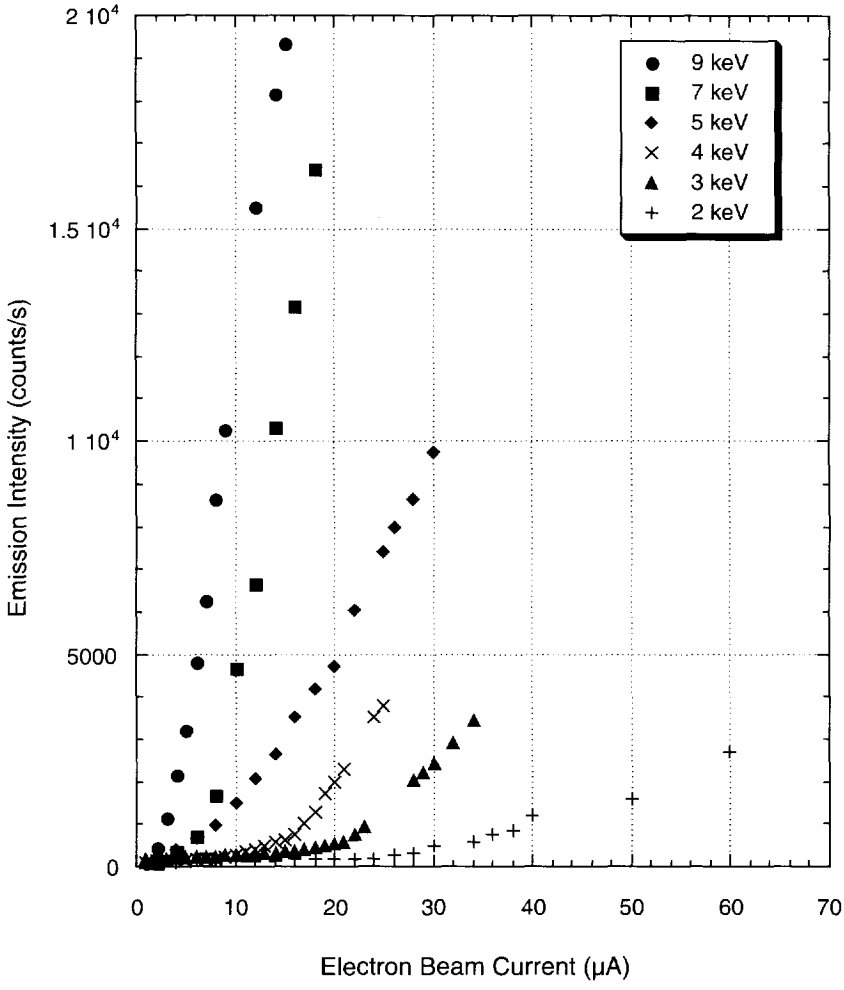

stimulated emission with feedback, or continuous-wave (cw) laser action.

Coherent back-scattering revealed that l^* was approximately half a wavelength, with a measured value of 311 ± 17 nm at 632.8 nm in perpendicular polarization and a similar value in parallel polarization, contrary to the general expectation from diffusion theory. The absence of speckle observed in above-threshold emission was also consistent with a subwavelength coherence length l_{coh}. In Fig. 6, the results to date for mean free transport distances $l^*(\lambda)$ are plotted versus λ. Only the results of coherent back-scattering experiments [15] in phosphor samples that exhibited emission with a clear threshold at the indicated wavelengths and had comparable particle sizes are included in the plot. These values were analyzed by taking into account reflection at the interface between the random medium and the vacuum [16]. No detailed consideration was given to possible systematic errors inherent in the back-scattering method by virtue of the sampling depth being on the same order as the transport length, a point we return to later. The l^* values increase between 362 and 633 nm, but all lie below the $l^* = \lambda$ curve. By

Fig. 5. Monte Carlo simulation of mean electron penetration in alumina versus incident energy. At each energy, results of many successive kinetic scattering calculations using the CASINO algorithm yielded data points fitted with a Gaussian curve to determine the mean depth, as illustrated in the inset for an incident energy of 10 keV.

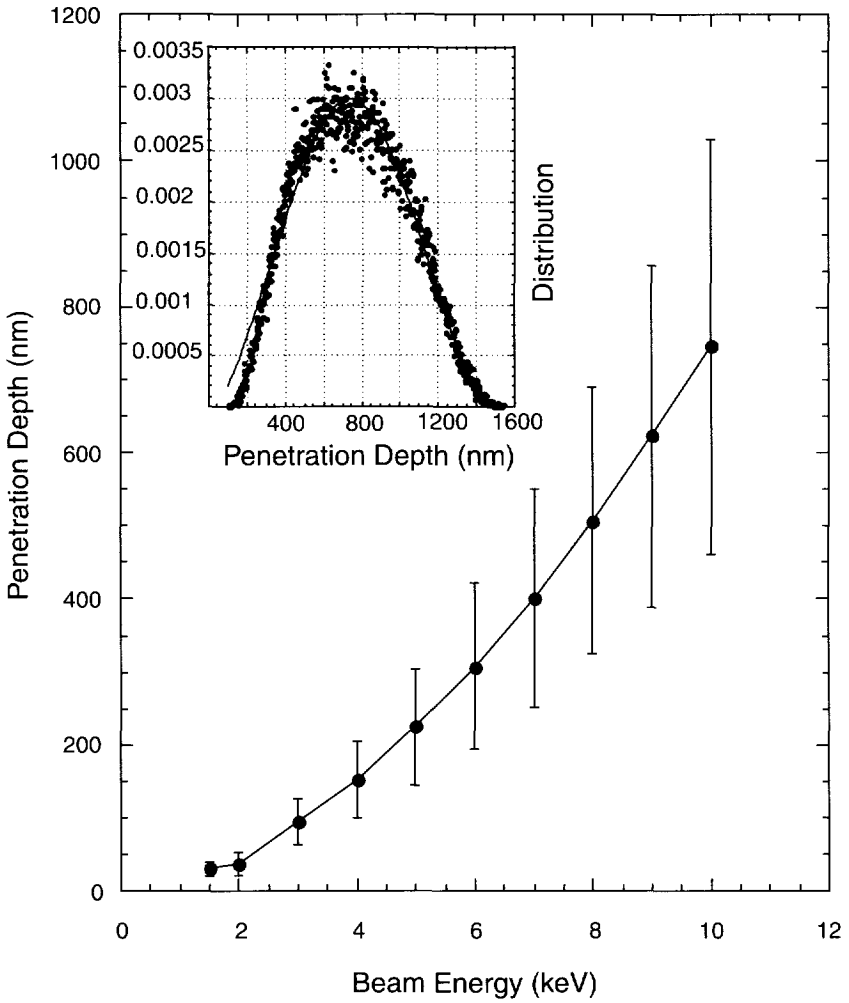

fitting a λ^{-4} dependence to the data, we estimate that the range over which strong localization may occur could extend over the entire visible spectral range in samples of this particle size, composition, and filling factor ($f \sim 0.4$).

We take the onset of cw laser action and other measurements presented here and in ref.1 as experimental evidence of strong localization of light in our powders, since very high internal reflection is required in (low gain) rare-earth systems to sustain efficient feedback. The results in Fig. 6 indicate that optical transport distances are limited to less than a half wavelength over a broad spectral range in dielectric nanopowders, and continuous laser action has been observed in our laboratory at three wavelengths between 350 and 650 nm in rare-earth-doped alumina powders. Since particle sizes and interparticle distances are too short in our samples for morphological resonances, we conclude that

Fig. 6. Values of l^* measured by coherent back-scattering for wavelengths at which stimulated emission thresholds were observed in dielectric nanophosphors. The continuous curve is a fit to a quartic wavelength dependence. Error bars are one sigma statistical estimates only, and do not include systematic errors discussed in the text. The straight line $l^* = \lambda$ is plotted for comparison.

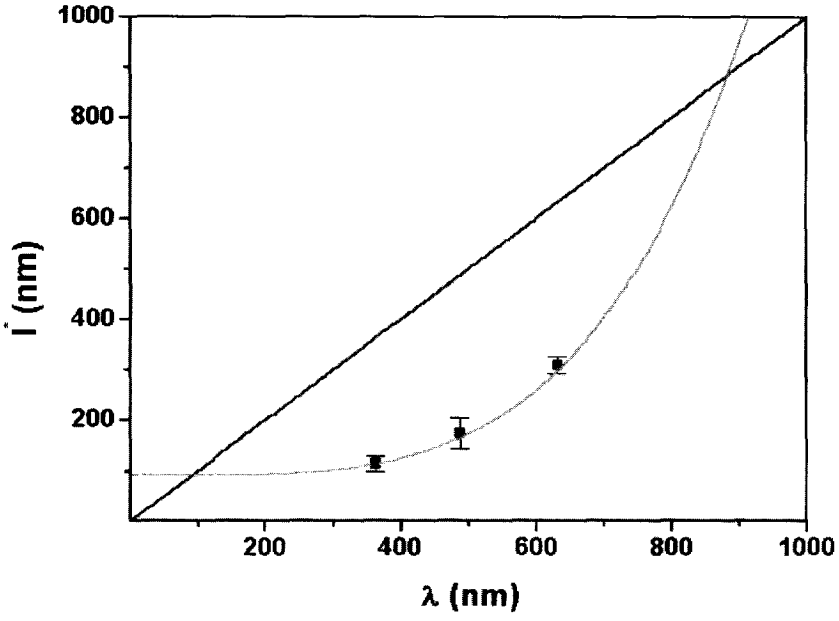

internal reflectivity that is near unity due to strong localization must account for the requisite feedback. This conclusion is also consistent with the *absence* of speckle, directionality, and discrete frequency (mode) structure in the output.

In Sect. 2, we argued that evanescent waves and strong localization manifest themselves under different conditions, namely, $r^* < \lambda/(2\pi\sqrt{(\omega_s^2/\omega^2) - 1}$ and $r^* < \lambda/2\pi$, respectively. These phenomena are closely related however. Both result in the appearance of nonpropagating waves. However, the dimensionality of the localization effect is different. Any degree of scattering in principle always produces evanescent waves and confinement with respect to the direction of propagation of an incident coherent plane wave [4], but this leads only to weak localization in three dimensions. It is easy to visualize that in finite-scattering media of thickness $L \ll l^*$, waves that would be evanescent and weakly localized on the scale of l^* (due to a correspondingly greater number of scattered field components) consist instead of limited superpositions of spatially oscillatory waves. Truncated distributions of oscillatory fields cannot sum to an exponentially small value everywhere outside a designated confinement region to yield strong localization in three dimensions. To guarantee complete confinement, the strong localization condition must require fields to be nonoscillatory on the scale of one wavelength. Interestingly, while our experimental values of l^* (in the samples that show threshold emission) are somewhat shorter ($l^* < \lambda/2$) than previous measurements, they still do not appear to satisfy (11). This raises questions about possible systematic errors in experimental determinations of l^* by back-scattering on subwavelength ranges, as well as relaxation of theoretical conditions necessary for strong localization arising from density-dependent interference effects. For example, with present theoretical understanding, l^* cannot be determined from back-scattering analysis without knowledge of the internal reflectivity R.

Yet R itself cannot be calculated unless interference effects are ignored. Future experiments will need to address such issues. It is appropriate to note that the relationships among the various statistical length scales l_{coh}, r^*, and l^* also need to be specified under conditions giving rise to evanescent waves — the very same conditions for which scalar wave theory is suspect. This calls for a vectorial approach.

Back-scattering experiments in the $l^* < \lambda$ limit are dominated by propagation characteristics at the input interface. This limitation biases the measurement of l^* in the range $l^* < \lambda$, through interfacial frustration of any Anderson transition in the layer contributing most to the signal. Shorter l^* values would be expected for fields excited by electrons at progressively greater depths from the surface of a strongly localizing medium. In this regard, our present measurements report the largest or "worst case" values of l^*. Also, (7) is strictly valid only at low densities of scatterers and our treatment of the local field factor L is no more rigorous than that of previous authors. This leaves considerable uncertainty about the modifications of localization condition (11) that may arise from correlated scattering. Pending further theoretical efforts and tensorial measurements of l^* in both back-scattering and transmissive geometries, we believe our experimental results to be consistent with and mediated by strong localization at visible wavelengths, because it is difficult to imagine how cw laser action could take place without the heightened internal reflectivity characteristic of the strong scattering regime.

A number of other interesting consequences arise in conjunction with negative permittivities from strong multiple scattering. When $l_{coh} < \lambda$, even phase conjugate pathways within a strongly localizing random medium are at best partially coherent. This is because the optical phase along designated paths is not well-defined when multiple reflections occur between two or more scatterers. This effect will strongly decrease the contrast ratio of the coherent back-scattering signal. Even though photonic atoms are stationary in space, their momentum properties are potentially interesting too. The observation of light emission in conjunction with continuous laser action in electrically-pumped nanopowders indicates that photons can be ejected from a localized electromagnetic field situated close to the surface of a random medium. Since the vibrational spectrum in the vicinity of the impurity atom(s) will in general be quantized due to short range order in the host, there is a finite probability that emission of the photonic atom system will be recoil-free. Hence we anticipate an unusual situation in which a spatially static electromagnetic *field* may emit propagating photons with or without vibrational frequency shifts. Direct determinations of the static nature of strongly localized light, its tensorial rest mass, and recoilless emission of photonic atoms are topics that await future experimentation.

There appears to be a close connection between inhibited spontaneous emission of atoms in quantum-confining [17] or photonic bandgap [18] structures and nonpropagating radiant emission of atoms in strongly scattering media. However, an important distinction is that in strongly scattering media *all modes* of space within the photonic atom radius (comprising the coupled impurity ion, host atoms and electromagnetic field in the $\sim (l^*)^3$ localization volume) are occupied in a nonradiative distribution, such that the constituent waves interfere destructively outside this volume. By contrast, atoms inhibited from spontaneous emission in microcavities have no modes available for occupation at all. Under the latter circumstances, ordinary atoms remain in the excited state and suppression of radiant transport is not an effect of randomized multimode or multiatom interference, as it is in photonic atoms.

Finally, as a consequence of finding that cw laser action is possible in highly scattering powders, we point out that photonic atom systems offer a new mechanism for energy storage. It is well known that in a cavity, which in the present instance is a random three-dimensional distributed feedback structure, the optical storage time τ depends on the ratio of stored energy to its dissipation rate, with the quality Q of the cavity being proportional to τ. Given that Q is large for cw lasers, we can surmise that once electromagnetic energy is released in the medium, it resides for a substantial length of time $\tau = Q/\omega$ deep in cw laser phosphors of the type described here. Volumetric, dynamic energy storage could be achieved by particle excitation, as shown here, or by stimulated Raman pumping at a wavelength just outside the pseudogap range [19]. The maximum storage time would be limited by the absorption coefficient α of the dielectric, amongst other factors, but its value unfortunately cannot be estimated

from the usual expression $\tau = (c_m \alpha)^{-1}$ for a uniformly distributed absorptive cavity loss, since this relies on the (undefined) phase velocity of light c_m in the medium. More detailed analyses will be needed to evaluate this application. However, photonic atoms clearly offer new challenges and opportunities, and the subject of strong localization should now be accessible to experimentation over a wide range of wavelengths.

Acknowledgements

The author is indebted to collaborators G. Williams, T. Hinklin, and R.M. Laine for all their experimental measurements and synthesis, to postdoctoral scholar B. Bayram for polarized back-scattering measurements, and to students S. Redmond, Bin Li, A. Harris, M. Rinkowski, J. Jiang, and X. Pan who also assisted with this research. Useful discussions are acknowledged with G.W. Ford and E. Leith. This research was funded by the Army Research Office (DAAD19-99-1-0229), the Air Force Office of Scientific Research (F49620-99-1-0158), and the National Science Foundation (DMR-9975542).

References

1. J. Goodman. Statistical optics. J. Wiley & Sons, New York. 1985. p. 206.
2. J.D. Jackson. Classical electrodynamics. 2nd ed. J. Wiley & Sons, New York. 1975. p. 285.
3. L.L. Foldy. Phys. Rev. **67**, 107 (1945); M. Lax. Rev. Mod. Phys. **23**, 287 (1951).
4. H.L. Fritsch and S.P. Lloyd. Phys. Rev. **120**, 1175 (1960).
5. M.P. van Albada and A. Lagendijk. Phys. Rev. B: Condens. Matter, **36**, 2353 (1987).
6. A.F. Ioffe and A.R. Regel. Prog. Semicond. **4**, 237 (1960).
7. D. Wiersma and A. Lagendijk. Phys. World, p. 33, January 1997.
8. N.M. Lawandy, R.M. Balachandran, A.S.L. Gomes, and E. Sauvain, Nature, **368**, 436 (1994).
9. M.A. Noginov, N.E. Noginov, H.J. Caulfield, P. Venkateswarlu, T. Thompson, M. Mahdi, and V. Ostroumov. J.O.S.A. B: **13**, 2024 (1996).
10. H. Cao, Y.G. Zhao, S.T. Ho, E.W. Seelig, Q.H. Wang, and R.P.H. Chang. Phys. Rev. Lett. **82**, 2278 (1999).
11. S. John. Phys. Rev. Lett. **53**, 216 (1984); Phys. Today, May 1991, p. 32.
12. S. John and G. Pang. Phys. Rev. A: At. Mol. Opt. Phys. **54**, 3642 (1996).
13. S. John and R. Rangarajan. Phys. Rev. B: Condens. Matter, **38**, 10 101 (1988).
14. A.C. Sutorik, S.S. Neo, T. Hinklin, R. Baranwal, D.R. Treadwell, R. Narayanan, and R.M. Laine. J. Am. Ceram. Soc. **81**, 1477 (1998); R.M. Laine, K. Waldner, C. Bickmore, and D. Treadwell. Double alkoxide monomers, oligomers, and polymers. U.S. Patent 5 614 596. March 1997.
15. M.P. van Albada and A. Lagendijk. Phys. Rev. Lett. **55**, 2692 (1985); P.E. Wolf and G. Maret. Phys. Rev. Lett. **56**, 1471 (1986).
16. J.X. Zhu, D.J. Pine, and D.A. Weitz. Phys. Rev. A, **44**, 3948 (1991); T.M. Nieuwenhuizen and J.M. Luck. Phys. Rev. E: Stat. Phys. Plasmas Fluids Relat. Interdiscip. Top. **48**, 560 (1993).
17. E.M. Purcell. Phys. Rev. **69**, 681 (1946); R.G. Hulet, E.S. Hilfer, and D. Kleppner. Phys. Rev. Lett. **55**, 2137 (1985).
18. E. Yablonovich. Phys. Rev. Lett. **58**, 2059 (1987); E. Yablonovich and T.J. Gmitter. Phys. Rev. Lett. **63**, 1950 (1989).
19. H.G. Winful and V. Perlin. Phys. Rev. Lett. **84**, 3586 (2000).